NASA-TM-111821

Three-Dimensional Viscous Flow Analysis of an Advanced Ducted Propeller Subsonic Inlet

C. Iek, D. R. Boldman, M. Ibrahim

Reprinted from

Journal of Propulsion and Power

Volume 11, Number 2, Pages 236–243

A publication of the
American Institute of Aeronautics and Astronautics, Inc.
370 L'Enfant Promenade, SW
Washington, DC 20024-2518

JOURNAL OF PROPULSION AND POWER
Vol. 11, No. 2, March–April 1995

Three-Dimensional Viscous Flow Analysis of an Advanced Ducted Propeller Subsonic Inlet

Chanthy Iek* and Donald R. Boldman†
NASA Lewis Research Center, Cleveland, Ohio 44135
and
Mounir Ibrahim‡
Cleveland State University, Cleveland, Ohio 44115

A time-marching Navier–Stokes code called PARC3D was used to study the three-dimensional viscous flow associated with an advanced ducted propeller (ADP) subsonic inlet at takeoff operating conditions. At a free-stream Mach number of 0.2, experimental data of the ADP inlet model indicated that the flow on the cowl windward lip remained attached at an angle of attack of 25 deg, became unstable at 29 deg, and separated at 30 deg. An experimental through-flow test study (without propeller) using another, but similar, inlet indicated that the separation occurred at an angle of attack a few degrees below the value observed when the inlet was tested with the propeller. This evidence showed that the propeller exerted a favorable effect on the inlet low speed and high angle-of-attack performance. A stationary blockage device was designed and tested with this latter inlet to simulate the propeller effect. The test data showed that the blockage device helped prevent the inlet flow from being separated at angle of attack a few degrees higher than the inlet through-flow, but was 1 deg lower than the inlet with the propeller. In the present numerical study, this flow blockage was modeled via a PARC3D computational boundary condition (BC) called the screen BC. The principle formulation of this BC was based on the "one-and-half dimensions" actuator disk theory. This screen BC was prescribed at the inlet propeller face station. Numerical results were obtained for inlet flow calculations with and without the screen BC. The results with the screen BC compared better with the ADP experimental test data than those obtained without the screen BC, particularly when the inlet flow separated.

Nomenclature

A = flow area, m^2
D = diameter, m
h = enthalpy per unit mass, J/kg
L = inlet length, m
M = Mach number
P = total pressure, Pa (N/m^2)
p = static pressure, Pa (N/m^2)
t = static temperature, K
W = mass flow rate, kg/s
X = distance, m
α = angle of attack, deg
δ = porosity, $(A_{pf} - A_{blk})/A_{pf}$
ε = pressure loss coefficient
η = normal to the surface
ρ = fluid density, kg/m^3
ϕ = circumference position, deg

Subscripts
c = captured
flx = flux
loc = local value on surface
pf = propeller face
pk = peak
sep = separation
0 = freestream

Presented as Paper 93-1847 at the AIAA/SAE/ASME/ASEE 29th Joint Propulsion Conference and Exhibit, Monterey, CA, June 28–30, 1993; received July 19, 1993; revision received March 3, 1994; accepted for publication July 26, 1994. This paper is declared a work of the U.S. Government and is not subject to copyright protection in the United States.

*Aerospace Research Engineer, Member AIAA.
†Aerospace Research Engineer, Retired Associate Fellow AIAA.
‡Associate Professor, Associate Fellow AIAA.

Introduction

A CRITICAL flow condition associated with a subsonic inlet is the onset of a flow separation during a steep climb for a takeoff operation. Flow separation has been a major concern for the design of a subsonic inlet. It should be avoided if at all possible for safety reasons, and to maintain a good propulsive efficiency. Up to the present time, the angle of attack α at which the inlet flow would separate has been determined by relying on experimental studies. Design and development then follow with a provision of an off-design operation by increasing the thickness of the inlet cowl lip. However, a thick lip would increase the inlet weight and would generate high drag at cruise. Also, it could result in a reduction of the critical flight Mach number beyond which the divergent drag rise would occur. Therefore, it is desirable to keep the inlet cowl lip as thin as possible for cruise, and as thick as necessary to keep the flow attached for takeoff. For a ducted propeller inlet the problem could become more complex because of the presence of the propeller as part of the propulsion front end flow ducting and directing system, especially at low speed. A design procedure that depends on experimental tests alone to achieve an optimized design of a subsonic inlet could be too costly, and so it may be beneficial to apply a CFD method to assist in the design process. For a low-speed and high-angle-of-attack flow, a CFD analysis needs to include the three-dimensional viscous effect if it is to predict the inlet aerocharacteristics, which may include a separated flow. For a ducted propeller system the inlet may need to be analyzed as part of an integrated system including the nacelle and the propeller since the latter may induce an effect that is substantial on the inlet performance.

A number of papers have been written about numerical studies of flows associated with through-flow and powered nacelles for takeoff and cruise operating conditions. Wie et al.[1] recently performed an inlet nacelle design and analysis study. This study explored the feasibility of designing a low

drag hybrid-laminar-flow nacelle by using a combination of an inverse Euler calculation and a two-dimensional flow prediction of laminar-turbulent boundary-layer transition. Valarezo[2] performed an analysis of a ducted propeller using a lower-order velocity panel method to study a circulation and pressure loading on propeller blades for different gap sizes between the blade tip and the shroud. Mendenhall and Spangler[3,4] conducted a numerical study of a ducted fan performance by using a potential flow method to estimate the aerodynamics at various α. Chen et al.,[5] Uenishi et al.,[6] and Hirose et al.[7] applied the Euler method to analyze flow-through and powered nacelles including the fan cowl, centerbody, and fan exit duct for axial flow and moderate values of α for takeoff and cruise flight conditions. For takeoff conditions, Chen analyzed a nonseparated flow condition associated with a powered nacelle at a freestream Mach number M_0 of 0.27, and α of 25 deg. Nakahashi[8] developed a hybrid method of finite difference and finite element to solve Reynolds-averaged Navier-Stokes RANS equations and Euler equations, respectively. This hybrid method was applied to predict three-dimensional nonseparated viscous flows associated with an inlet nacelle for takeoff and cruise conditions. The validity of this study was assessed based on the computational results only. Srivastava[9] applied a hybrid implicit-explicit unsteady scheme to solve the Euler equations to obtain prediction of the aeroelastic characteristics of a ducted propeller at cruise. Hall and Delany[10] developed a three-dimensional Euler-based computer code to predict flow characteristics associated with a single-stage ducted propeller for axial and high α freestream flows. Boldman et al.[11] applied a panel method with a built-in compressibility correction to evaluate several ducted propeller inlets for takeoff conditions. By employing an empirical method based on the inlet cowl peak Mach number M_{pk}, the results could provide an indication of the angle of attack at which the inlet flow would separate. The panel method did not account for the propeller effect. However, without separation the comparison with the test data showed that the potential flow provided a good prediction of the static pressure distribution on the inlet cowl windward and leeward sides.

Potential flow and Euler analyses are generally fast for computer turnaround time solutions. Both are capable of providing good prediction of flows associated with inlet nacelles, but are limited to certain flow conditions. Potential flow calculations are limited to a subsonic nonseparated flow. Euler calculations can handle both subsonic and supersonic flows, but also are limited to a nonseparated flow.

As part of the advanced ducted propeller (ADP) research program, NASA Lewis Research Center (LeRC) and Pratt and Whitney (P&W) conducted experimental and numerical studies of aerodynamics for a takeoff operation associated with several inlet models. Each was tested with a propeller for an ADP test, and one was selected to be tested without the propeller for a through-flow test. The test data from these studies[11,12] showed that the inlet through-flow separated at an α value a few degrees lower than that of the ADP inlet flow. This evidence indicated that the propeller exerted a favorable effect on the inlet low-speed and high-angle-of-attack aeroperformance. The nature of this effect was not readily comprehensible due to the complexity of the flow interaction between the propeller and the inlet mainstream. However, knowledge of this flow interaction could help advance the design methodology to incorporate the propeller effect for the consideration of the inlet internal flow performance. Subsequently, in a later portion of the through-flow test, the inlet was tested with a stationary blockage device installed at the propeller face location to simulate the propeller blockage effect on the inlet internal flow. The test results showed that the blockage device was able to sustain the inlet flow from being separated up to 1 deg below the separation angle of attack α_{sep} shown in the ADP test data. This evidence indicated that the propeller blockage, among others such as swirl and suction, played a significant role on the inlet performance.

The objective of the present numerical study was to apply an existing three-dimensional RANS flow solver called the PARC3D code to analyze the flow characteristics associated with an ADP subsonic inlet. Flow calculations were made for a freestream flow $M_0 = 0.2$, at three different angles of attack, $\alpha = 25$, 29, and 30 deg. Grid configuration of the ADP inlet did not include modeling of the actual propeller geometry, instead, a computational BC was applied to simulate the blockage effect of the propeller.

Experimental Background

In 1990, NASA LeRC and P&W jointly conducted an experimental study to develop technology for a low noise/low drag ADP propulsion system. Several inlet designs were tested with a propeller for an ADP simulator test in the NASA LeRC's 9- × 15-ft Low Speed Wind Tunnel. The ADP test data were taken for a nominal M_0 of 0.2, α from 0 to 35 deg, and a propeller speed range from 7500 to 12,000 rpm. The inlet captured mass flow rate W_c ranged from 14.06 to 21.12 kg/s. Figure 1 shows schematics of two ADP inlets. The one shown in Fig. 1a was called the baseline design, and the other shown in Fig. 1b was called the midlength design. The two inlets were very similar, the only difference was that the baseline cowl length was about 5.0 cm longer than the midlength cowl.

Shortly after the ADP wind-tunnel test was completed, NASA LeRC further investigated the through-flow aeroperformance of the baseline inlet shown in Fig. 1a. The test was conducted using the United Technologies Research Center's 10 × 15-ft Subsonic Wind Tunnel. The effect of the propeller on the ADP inlet could be determined by comparing the data from the through-flow test with the data from the ADP test. Figure 2 shows the through-flow static pressure distributions on the cowl windward side for $M_0 = 0.2$ and $W_c = 17.41$ kg/s. At $\alpha = 25$ deg, the inlet flow was attached as indicated by a large expansion and diffusion around the highlight (Fig. 2a). At $\alpha = 26$ deg, the flow was fully separated (Fig. 2b) as indicated by a relatively small expansion and practically no diffusion around the highlight. The ADP data that is shown in Fig. 3c, in open circles, indicated that the baseline inlet separated at $\alpha = 30$ deg. The difference in the values of α_{sep} shows that the propeller exerted a favorable effect on the inlet aeroperformance. This propeller effect was further investigated in the later portion of the test. The method used in this investigation was to partially block the inlet internal flow by employing a stationary blockage device installed at the propeller face location. Figure 3 shows a comparison of static

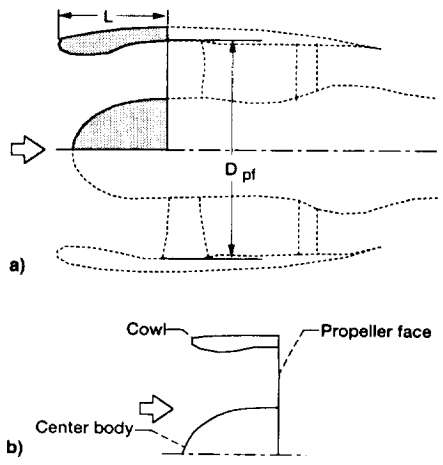

Fig. 1 Comparison of two ADP inlet configurations: a) baseline, $L/D_{pf} = 0.5$ and b) midlength, $L/D_{pf} = 0.4$.

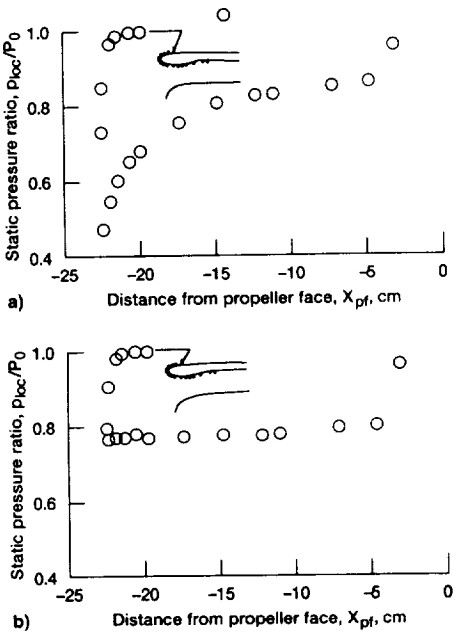

Fig. 2 **Baseline inlet experimental static pressure distributions on the cowl windward for through-flow at M_0 = 0.2 and W_c = 17.41 kg/s: a) before separation, α = 25 deg and b) after separation, α = 26 deg.**

pressure distributions from the baseline inlet tested with the blockage device and from the ADP test for M_0 = 0.2 and W_c = 17.41 kg/s. At α = 28 deg (Fig. 3a), the two static pressure distributions are nearly the same, indicating that the effect induced by the blockage device was similar to that generated by the propeller. At α = 29 deg (Fig. 3b), the static pressure distribution from the inlet with the blockage device shows that the flow was separated, but the ADP data shows that the flow was still attached. At α = 30 deg (Fig. 3c), both static pressure distributions are similar and indicate that the inlet flows in both cases were separated. A comparison of Figs. 2 and 3 shows that the inlet with either the propeller or the stationary blockage device performed better than the inlet through-flow in terms of high-angle-of-attack operation. This contribution by the propeller to the inlet angle-of-attack capability could be significant for an advanced subsonic inlet design where a compromise needs to be made between a thin cowl lip to achieve low drag and a thick cowl lip to prevent lip separation.

The comparison in Fig. 3 shows that the stationary blockage device was capable of simulating the effect of the propeller to within 1 deg of the inlet α_{scp}. In the present numerical study, the propeller blockage effect was simulated by means of a CFD boundary condition (BC) called the screen BC. The fundamental formulation of this boundary condition was based on the one-and-half dimensions actuator disk theory. The inlet used for this CFD study was the midlength design shown in Fig. 1a. Note that only the baseline inlet and not the midlength

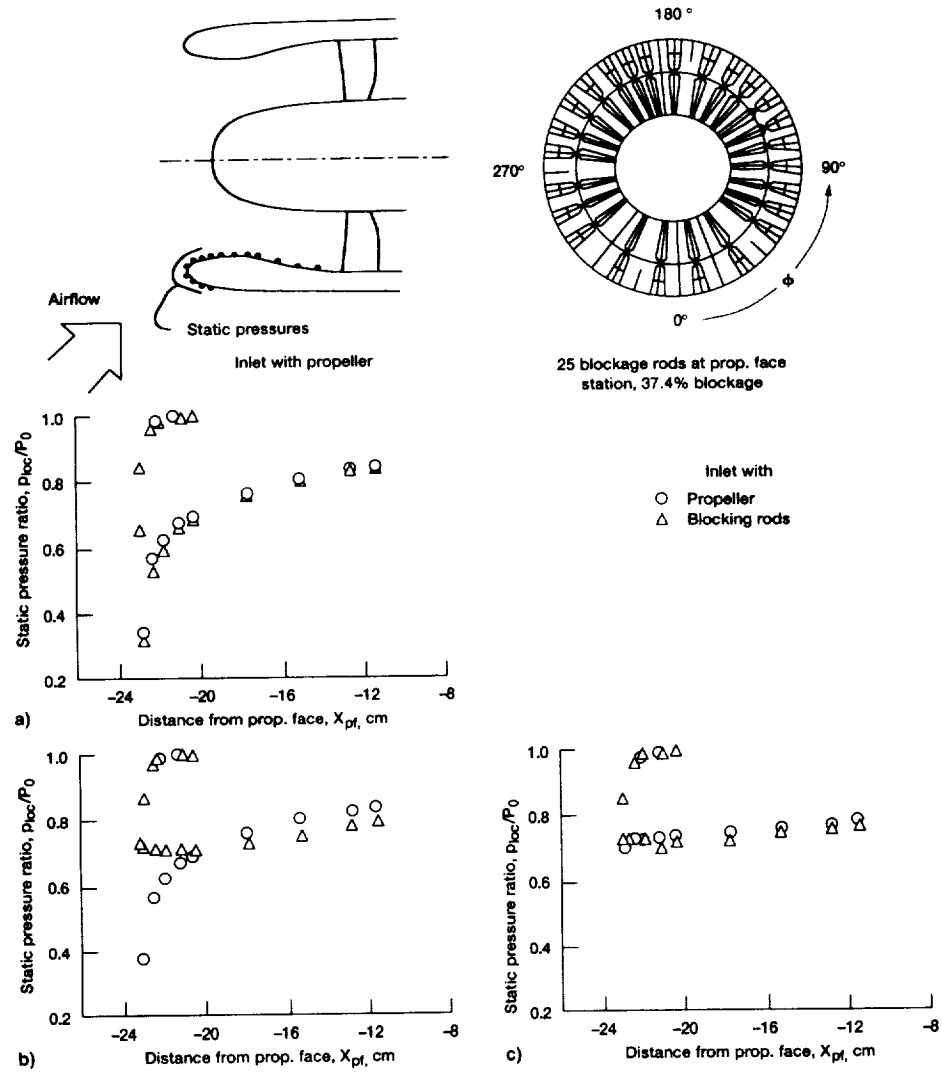

Fig. 3 **Comparison of baseline inlet windward static pressure distributions from experiments for M_0 = 0.2 and W_c = 17.41 kg/s. α = a) 28, b) 29, and c) 30 deg.**

was tested in the through-flow/propeller blockage simulation study. However, the ADP data showed that aeroperformances of both inlets were very similar. Therefore, if the midlength inlet had been used in this test study, the aeroperformance data would be very similar to the data obtained with the baseline inlet as shown in Figs. 2 and 3.

Computations

PARC3D Code

The PARC3D code was selected for this numerical study. It was a three-dimensional, multiblock Reynolds averaged Navier-Stokes (RANS) solver. It utilizes the central differencing scheme on a generalized curvilinear coordinate system. The turbulence model used in the code is the Baldwin-Lomax model. The PARC3D code was capable of computing flows about complex geometries with computational boundary conditions that could be specified on any portion of the grid surfaces. The code incorporated a semiautomatic time-step control function that could help to maintain the stability for the flow solution being iteratively calculated. Additional details about the code can be found in Ref. 13.

Computational Grid

A general purpose CFD grid generating tool called GRID GEN[14] was utilized to generate the multiblock grid for this study. An earlier CFD study by Iek et al.[15] for a similar flow calculation shows that using an embedded C-grid block around the cowl lip improved the results significantly. For this study this grid embedding method was also emloyed. Grid lines were generated using a combination of the Bazier's curve fit and the transfinite interpolation. Grid clustering and orthogonality at and near the wall boundaries were generated using the algebraic and the elliptic solvers to provide a streamwise distibution of $y+$ between 2–5. The total number of grid points was 7.6×10^5.

Computational Boundary Conditions

Figure 4 shows computational BCs applied at various sections of the grid. The flowfield throughout the computational domain was calculated in viscous mode. The external portion of the flowfield terminated at the nacelle trailing edge; therefore, the computational results did not account for the effect of the plume aft of the nacelle body. According to an analysis study by Uenishi,[6] the effect of the plume propagates upstream, but not far enough to influence the inlet internal flow performance that was the main subject in this study. The nacelle surrounding flowfield was calculated using the computational freestream BC. At the inlet nacelle surface, the no-slip BC was specified. The screen BC and the mass BC were specified at the inlet propeller face and the nacelle exit, respectively. Mathematical formulations of freestream, no-slip, and mass BCs are reported in Ref. 13.

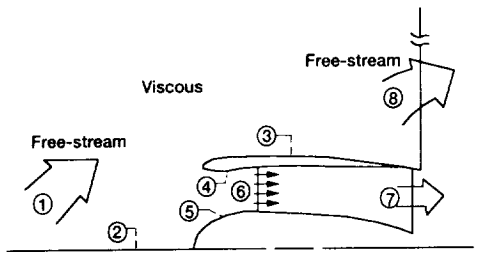

	Boundaries	BC's	Prescribed variables
1, 8	Far field	Free-stream	M_0, α
2	Centerline	Singular	
3, 4, 5	Cowl & center body surfaces	No-slip wall	
6	Propeller face station	Screen	δ
7	Exit	Mass flux	W_{flx}

Fig. 4 PARC BCs applied in analyses using screen BC at the propeller face.

Screen BC

This BC was developed based on the one-and-half dimensions actuator disk theory by Horlock.[16] It imposed a flow disturbance that behaves similar to a wire-mesh screen. When a flow passes through a screen there is some pressure loss. The magnitude of this loss depends on the approaching flow velocity and the screen porosity. In order to compute the flow downstream of the screen, a pressure loss coefficient ε was determined based on an experimental study by Pinker and Herbert.[17] The fundamental governing equations for the screen BC can be written

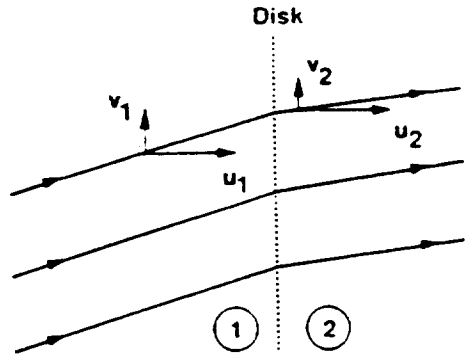

$$\rho_1 u_1 = \rho_2 u_2 \quad \text{continuity}$$

$$p_1 + \rho_1 u_1^2 = p_2 + \rho_2 u_2^2 \quad x\text{-momentum}$$

$$\rho_1 u_1 v_1 = \rho_2 u_2 v_2 \Rightarrow v_1 = v_2 \quad y\text{-momentum}$$

$$h_1 + (u_1^2 + v_1^2)/2 = h_2 + (u_2^2 + v_2^2)/2$$

$$\Rightarrow h_1 + u_1^2/2 = h_2 + u_2^2/2 \quad \text{energy}$$

$$p_1/\rho_1 t_1 = p_2/\rho_2 t_2 \quad \text{state}$$

$$\varepsilon = (p_1 - p_2)/(0.5\rho_1 u_1^2) \quad \text{pressure loss coefficient}$$

The pressure at the downstream side of the screen cannot be determined analytically and is calculated based on the value of pressure loss coefficient. The screen BC requires a specification of the screen porosity δ. The value of δ is zero for a 100% flow blockage, and unity for a 0% flow blockage. From Ref. 12 based on a one-dimensional flow calculation, an amount of flow blockage that was effective in simulating the propeller blockage effect induced a propeller face Mach number between 0.8–1.0. Based on this reference, a propeller face Mach number of 1.0 was selected to determine the value of δ. And by using the value of W_c of 21.12 kg/s, δ was calculated to be 0.72. Note that the propeller face Mach number of 1.0 was chosen simply for simplicity.

The screen BC is analogous to a passive blockage device that does not have any suction capability of generating airflow through the inlet. In order to simulate a certain amount of mass flow, a mass BC is needed downstream of the screen boundary. As shown in Fig. 4, the screen BC was prescribed at the propeller face (BC6) and a mass BC was at the inlet exit (BC7). For the inlet through-flow simulation, the inlet flow calculation was made simply without using the screen BC and only with the mass BC.

Results and Discussion

The PARC3D flow calculations were made to analyze flow associated with the ADP midlength inlet (Fig. 1) for M_0 of 0.2, W_c of 21.12 kg/s, and α of 25, 29, and 30 deg. The selection of these three values of α was based on the ADP experimental test data as shown in Ref. 11, which indicate that the inlet flow was attached at α = 25 deg, unstable at α = 29 deg, and separated at α = 30 deg. For α = 25 and 29 deg, the flow calculations were made with and without the screen BC, and for α = 30 deg, the calculation was made only with the screen BC. The computational results were evaluated by comparing the numerical results with the ADP experimental test data for the midlength inlet.

Angle of Attack of 25 Deg—No Separation

Figure 5 shows the inlet flow Mach contours obtained from the PARC3D calculations with and without the screen BC at the inlet propeller face. The Mach contours show flow characteristics on the inlet center plane comprised of the windward (lower half) and the leeward (upper half) sides for M_0 = 0.2, α = 25 deg, and W_c = 21.12 kg/s. Without the screen BC, Fig. 5a shows the flow stagnation points on the leeward and the windward sides are located at the highlight and on the external cowl surface just aft of the highlight, respectively. On the cowl windward side around the inlet lip, the flow experienced a rapid expansion and diffusion. In the expansion part the flow developed a local supersonic flow with a local peak Mach number M_{pk} of 1.27, and in the diffusion part the flow speed locally reduced from M_{pk} of 1.27 to an M_{loc} of 0.53 just upstream of the propeller face plane. On the leeward side near the cowl highlight, the flow expanded and diffused at a much slower rate than that on the windward side. As a result, the boundary-layer thickness on the cowl leeward side is considerably thinner than that on the cowl windward side. The stagnation point on the centerbody is slightly off the centerline, and the boundary-layer thickness on the upper surface is similar to that on the lower surface. With the screen BC, the flowfield in Fig. 5b shows similar characteristics to those in Fig. 5a upstream of the propeller face. A comparison of the Mach contours Figs. 5a and 5b shows the effect of the screen BC on the inlet internal flowfield in vicinity of the propeller face plane. The screen apparently induced a disturbance that caused a redistribution of the flowfield to become uniform in terms of Mach number. This disturbance behaved like a blockage in the inlet flow stream. On the windward side the screen induced a perturbation in the boundary layer resulting in a reduction of the boundary-layer thickness. On the cowl leeward side and on the centerbody, a similar perturbation is apparent, but the results are not obvious since the boundary layers there are very thin.

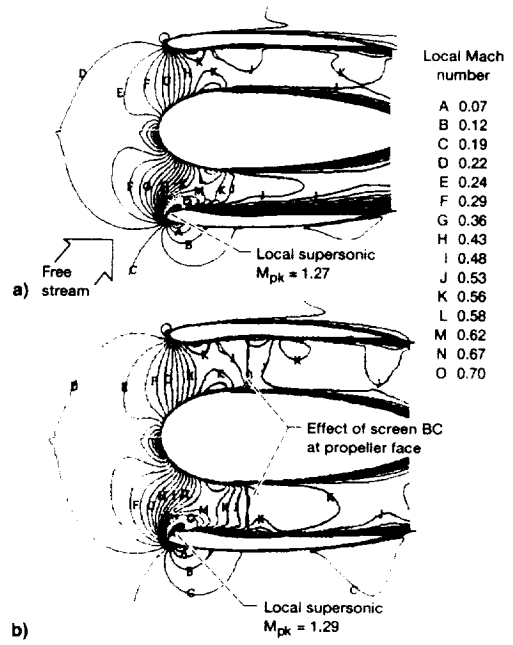

Fig. 5 Mach contours over the inlet center plane for M_0 = 0.2, α = 25 deg, and W_c = 17.41 kg/s: a) with and b) without screen BC.

Figure 6 shows a comparison of inlet cowl static pressure distributions of the ADP experimental data with computational results. On the windward side (Fig. 6a), the calculated pressure distributions with and without the screen BC are practically the same. The two predicted static pressure distributions agree well with the test data. On the leeward side (Fig. 6b), a good agreement is obtained on the external cowl surface, but the predicted distribution on the internal cowl surface is slightly lower than the test data. The effect of the screen BC on the inlet flow, as shown in the Mach contour plots, did not have a significant impact on the cowl axial static pressure distribution upstream of the propeller face.

The airflow on the windward lip did not separate at α = 25 deg. Nonetheless, this inlet flow condition served as a test case to study the flow characteristics resulting from PARC3D calculations of the inlet with and without using the screen BC. Evaluation of the computational results indicated that the calculations predicted the inlet flow characteristics reasonably well. However, it has not yet been demonstrated how well this computational blockage could simulate the propeller blockage effect as compared to the effect induced by the stationary blockage device used with the baseline inlet (Figs. 2 and 3). To further assess the effectiveness of the screen BC, subsequent calculations were carried out with two angles of attack involving inlet unstable (about to separate) and separated flows, respectively, as shown in ADP test data discussed in Ref. 11.

Angle of Attack of 29 Deg—Unstable Flow

Figure 7 shows streamwise Mach contours on the inlet vertical center plane. The flow characteristics for α = 29 deg

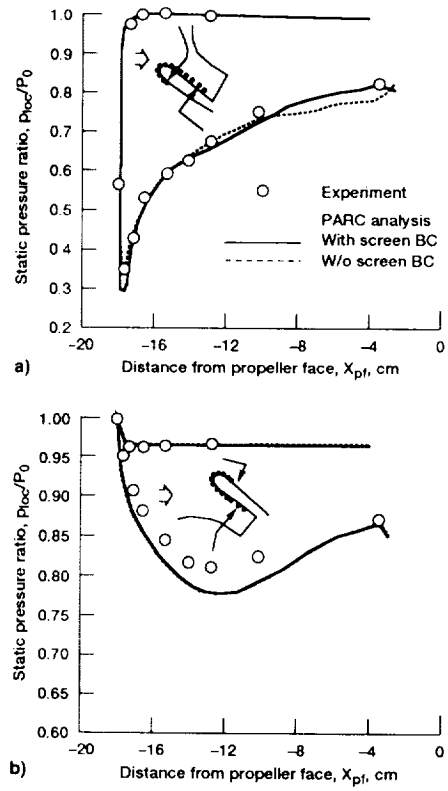

Fig. 6 Comparison of static pressure distributions between analyses and experiment for M_0 = 0.2, α = 25 deg, and W_c = 17.41 kg/s: a) windward side, ϕ = 0 deg and b) leeward side, ϕ = 180 deg.

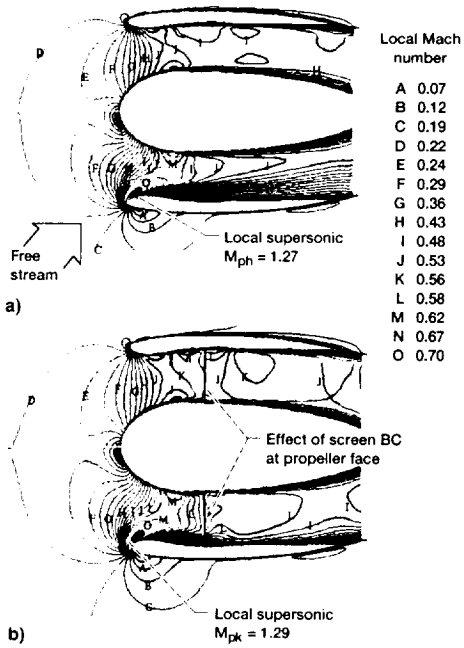

Fig. 7 Mach contours over the inlet center plane for M_0 = 0.2, α = 29 deg, and W_c = 17.41 kg/s: a) with and b) without screen BC.

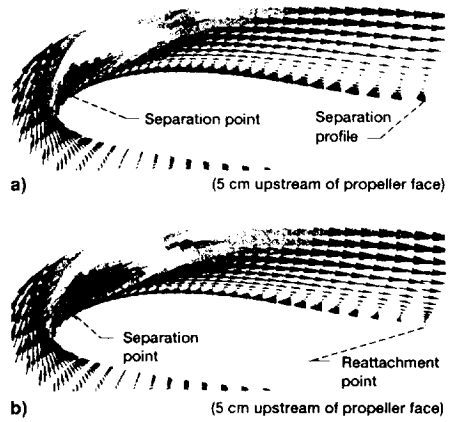

Fig. 8 Axial velocity vector distributions for M_0 = 0.2, α = 29 deg, and W_c = 17.41 kg/s: a) with and b) without screen BC.

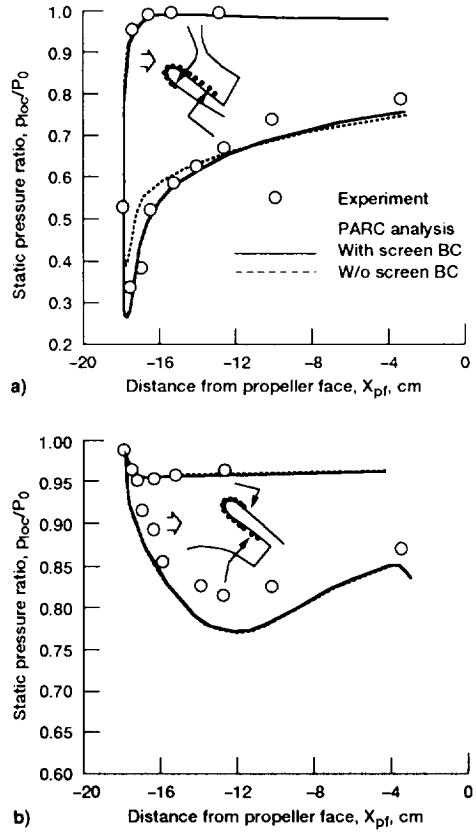

Fig. 9 Comparison of static pressure distributions between analyses and experiment for M_0 = 0.2, α = 29 deg, and W_c = 17.41 kg/s: a) windward side, ϕ = 0 deg and b) leeward side, ϕ = 180 deg.

are similar to some aspects and differences from those obtained for α = 25 deg that were shown in Fig. 5. The similarity includes locations of stagnation points on cowl windward and leeward sides, flow expansion and diffusion, and the blockage effect induced by the screen BC at the propeller face. And the differences include the local peak Mach number and the boundary-layer thickness particular on the cowl windward side. Without the screen BC, the local peak Mach number on the cowl windward highlight decreased from M_{pk} = 1.27 at α = 25 deg (Fig. 5a) to M_{pk} = 1.25 at α = 29 deg (Fig. 7a). With the screen BC, the peak Mach number increased from M_{pk} = 1.29 (Fig. 5b) to M_{pk} = 1.35 (Fig. 7b). The reduction in the peak Mach number for the case without the screen BC, based on Ref. 11, suggests that the flow at α = 29 deg may have separated. Flow separation in fact did occur as shown in the velocity vector distributions on the inlet cowl windward side in Fig. 8. Both calculations with and without the screen BC predicted a lip-type flow separation that occurred upstream near the highlight and continued downstream. Without the screen BC, Fig. 8a shows the flow separation extended past the propeller face. With the screen BC, Fig. 8b shows the flow reattached about 5 cm upstream of the propeller face and remained attached downstream of that. This evidence reveals that the blockage effect induced by the screen BC was capable of suppressing the separation before the flow reached the screen.

Figure 9 shows a comparison of static pressure distributions of the ADP experimental data with computational results for M_0 = 0.2, α = 29 deg, and W_c = 21.12 kg/s. On the windward side (Fig. 9a), the pressure distribution from the calculation with the screen BC compares more favorably with the test data than the results obtained from the calculation without the screen BC, particularly around the inlet cowl highlight. On the leeward side (Fig. 9b), the two predicted pressure distributions are similar and compare favorably with the test data on the inlet external surface, but are slightly off on the internal surface.

The ADP experimental data[11] indicated that the midlength inlet flow fully separated at α = 30 deg. The inlet through-flow (without any blockage) was expected to separate a few degrees earlier. This was substantiated by the experimental data associated with the baseline inlet (Figs. 2 and 3). The PARC3D calculation without the screen BC (through-flow simulation) predicted cowl lip separation with the midlength inlet at α = 29 deg, which concurs with the experimental evidence. The level of the separation cannot be assessed due to the lack of flowfield experimental data. The PARC3D calculation with the screen BC also predicted inlet lip separation, but the flow reattached about 5.0 cm upstream of the propeller face where the screen BC was specified. The blockage effect induced by the screen BC appears to agree with the effect induced by the stationary blockage rods used with the baseline inlet (Figs. 2 and 3).

Angle of Attack of 30 Deg—with Separation

The inlet flow calculation for this case was made only with the application of the screen BC to study its blockage effect on the inlet internal flow, particularly on the windward side where separation was expected to occur. Figure 10 shows

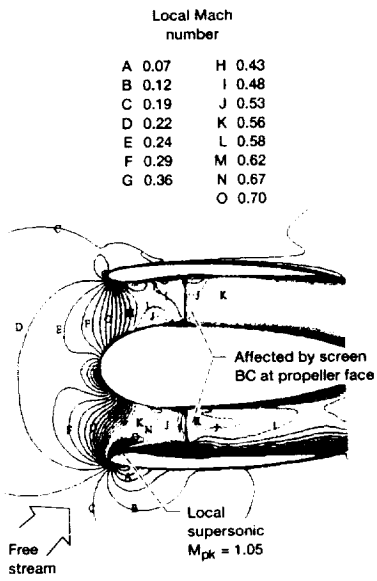

Fig. 10 Mach contours over the inlet center plane for M_0 = 0.2, α = 30 deg, and W_c = 17.41 kg/s.

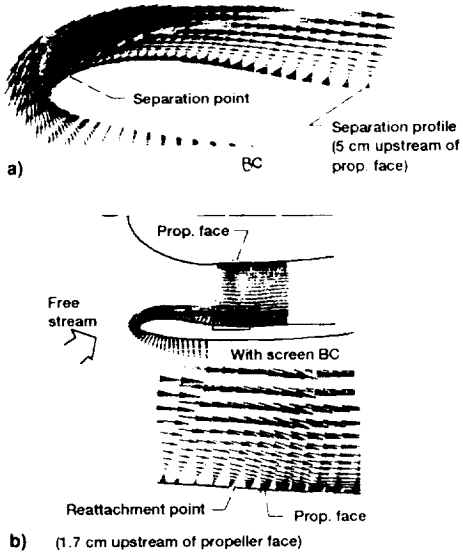

Fig. 11 Axial velocity vector distributions for M_0 = 0.2, α = 30 deg, and W_c = 17.41 kg/s: a) on the cowl windward side and b) axial velocity vectors distribution around the propellar face.

Mach contours from the PARC3D calculation for M_0 = 0.2, α = 30 deg, and W_c = 21.12 lb/s. On the windward side around the cowl lip, the inlet flow went through a rapid expansion and a quick diffusion similar to flow characteristics discussed earlier for α of 25 and 29 deg. In the expansion part the local peak Mach number is M_{pk} = 1.05. A comparison with the peak Mach number for α = 29 deg (Fig. 7b) shows that M_{pk} dropped from 1.35 to 1.05 as the angle of attack increased from α = 29–30 deg. This reduction in the peak Mach number indicates that the inlet flow at α = 30 deg separated, and the level of the separation was larger than that at α = 29 deg. Figure 11a shows the flow separation on the cowl windward side starting from the highlight, and extended past the location 5.0 cm upstream of the propeller face plane where the separated flow reattached for α = 29 deg in Fig. 8b. Figure 11b shows that separation ceased and the flow reattached at the location 1.7 cm upstream of the propeller face plane. The screen BC induced a blockage effect that forced the approaching flow to become uniform. It also induced a perturbation in the flow boundary layer, resulting in

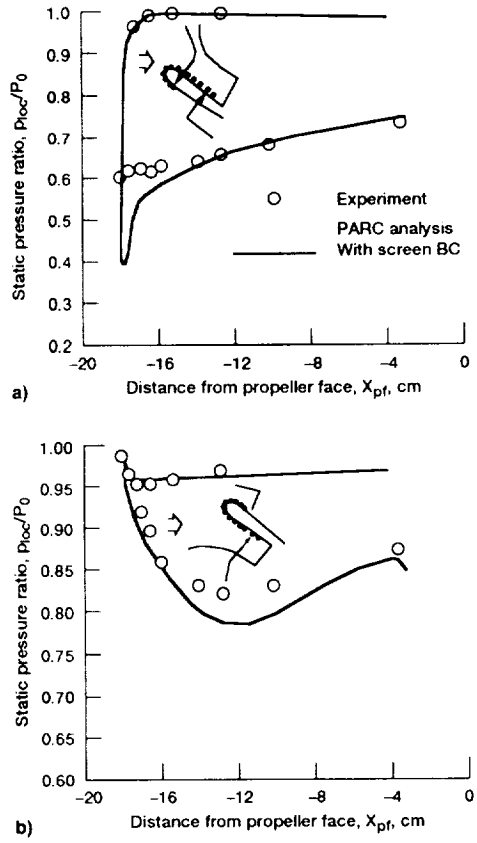

Fig. 12 Comparison of static pressure distributions between analysis and experiment for M_0 = 0.2, α = 30 deg, and W_c = 17.41 kg/s: a) windward side, ϕ = 0 deg and b) leeward side, ϕ = 180 deg.

a reduction in the boundary-layer thickness a short distance downstream of the screen.

Figure 12 shows a comparison of static pressure distributions of the ADP experimental data with the computational results. The test data on the windward side shows that the inlet flow fully separated as indicated by the pressure distribution towards the highlight, showing the flow experienced a considerably smaller expansion than the two previous cases for α of 25 and 29 deg. Downstream of the highlight, it experienced practically no diffusion. With the exception of around the highlight region, a comparison on the cowl windward side shows that the predicted static pressure distribution agrees with the experimental data on the external and internal surfaces. Around the highlight the analysis predicted a peak static pressure value that is significantly lower than the experimental data. The reason for this difference has not been determined. The comparison on the inlet leeward side shows good agreement on the external surface and at the highlight, but a small difference appears on the internal surface.

Future Study

A propeller is a rotating device in a flow medium, therefore, it generates a centrifugal force on and adds energy to the flow. The effects induced by the propeller on oncoming subsonic flow include blockage, swirl, and suction. In this study the screen BC only induced a blockage effect on the flowfield. As a result of this blockage effect, a perturbation was generated in the flow boundary layer. This blockage effect was passive and generates neither swirl nor suction on the oncoming flow. Instead of adding energy to the flow, the screen BC created a momentum deficit in the flowfield. Therefore, the blockage effect was the only commonality between the propeller and the screen. The suction in this numerical study was generated using a mass BC downstream of the screen. Therefore, the inlet flow calculation using the screen BC to simulate

the propeller effect still neglected the swirl effect of the propeller. A suggestion for future related work would be to include the swirl effect into the analysis in addition to the blockage effect, e.g., the screen BC. The most viable location for this swirl effect is at the propeller face plane.

Conclusions

This article summarizes a research study done by a cooperative effort of NASA LeRC and P&W to expand the technology base for an advanced ducted propeller system, specifically pertaining to the effect of the propeller on the inlet aeroperformance at a low speed takeoff operating condition. The study involved an experimental test of aeroperformance and a numerical analysis of three-dimensional viscous flow associated with an ADP inlet.

The experimental test data showed that the ADP inlet flow remained attached up to an angle of attack a few degrees higher than that of the inlet through-flow (without the propeller). The inlet was tested with a stationary blockage device installed at the propeller face location. The test data showed that the blockage device induced an effect that was similar to that generated by the propeller on the inlet aeroperformance at a low speed and a high angle of attack. This evidence indicated that the blockage effect induced by the propeller, among others such as swirl and suction, could play a major role on the inlet internal flow performance.

In the numerical analysis, the propeller blockage was simulated in terms of a computational boundary condition called the screen BC that was developed based on the one-and-half dimensions actuator disk theory. The screen BC was incorporated in a three-dimensional RANS flow solver called the PARC3D code. The code was used for the ADP inlet analysis for flow conditions including $M_0 = 0.2$, $\alpha = 25$, 29, 30 deg, and $W_c = 21.12$ kg/s. The three values of α were selected based on an indication by the ADP test data for attached, unstable, and separated flows, respectively. Three flow calculations for individual α were made with the screen BC imposed at the propeller face plane and a mass BC imposed downstream at the nacelle exit plane to simulate the required amount of airflow through the inlet. Two additional flow calculations were made without the screen BC, but with the mass BC to simulate the inlet through-flow. The computational results showed the screen BC induced a blockage effect that forced the inlet flow to become uniform at and generated a perturbation in the boundary layer around the location where the screen BC was prescribed. The general flow characteristics associated with the inlet for each value of α for calculations with and without the screen BC could be described as follows:

1) At $\alpha = 25$ deg, the predicted inlet flow was attached as indicated by the ADP test data. Both flow calculations with and without the screen BC provided static pressure distributions that were in good agreement with the test data.

2) At $\alpha = 29$ deg, the predicted inlet flow was separated, but the ADP test data showed the inlet flow was unstable or just at the start of separation. The separation point was near the highlight. Without the screen BC the separation persisted downstream past the propeller face location. With the screen BC the separation ceased and a reattachment point began a short distance, about 5.0 cm, upstream of the propeller face plane. As a result, the predicted static pressure distribution associated with the latter compared better with the ADP test data than the former.

3) At $\alpha = 30$ deg, the predicted inlet flow was separated as indicated by the ADP test data. For this case the flow calculation was made only with the use of the screen BC. The calculated flow reattached a short distance 1.7 cm upstream of the propeller face plane. The predicted static pressure distributions were in good agreement with the test data, except in the vicinity of the highlight where the prediction showed a drop in static pressure substantially lower than that of the test data. The cause for the difference had not yet been determined.

References

[1]Wie, Y. S., "Design of a Hybrid Laminar Flow Control Engine Nacelle," AIAA Paper 90-0400, Jan. 1992.

[2]Valarezo, W. O., "Calculation of Subsonic Shrouded Propeller Flows," AIAA Paper 90-0029, Jan. 1990.

[3]Mendenhall, M. R., and Spangler, S. B., "Theoretical Study of Ducted Fan Performance," NASA CR-1494, Jan. 1970.

[4]Mendenhall, M. R., and Spangler, S. B., "A Computer Program for the Prediction of Ducted Fan Performance," NASA CR-1495, Feb. 1970.

[5]Chen, H. C., Yu, N. J., and Rubbert, P. E., "Flow Simulation for General Nacelle Configurations Using Euler Equations," AIAA Paper 83-0539, Jan. 1983.

[6]Uenishi, K., Pearson, M. S., Lehnig, T. R., and Leon, R. M., "CFD-Based 3D Turbofan Nacelle Design System," AIAA Paper 90-3081, Aug. 1990.

[7]Hirose, N., and Asai, K., "Euler Flow Analysis of Turbine Powered Simulation and Fanjet Engine," *Journal of Jet Propulsion*, Vol. 7, No. 6, 1991, pp. 1015–1022.

[8]Nakahashi, K., "FDM—FEM Zonal Approach for Viscous Flow Computations over Multiple-Bodies," AIAA Paper 87-0604, Jan. 1992.

[9]Srivastava, R., "An Unsteady Euler Scheme for the Analysis of Ducted Propellers," AIAA Paper 92-0522, Jan. 1992.

[10]Hall, E. J., and Delany, R. A., "3D Euler Analysis of Ducted Propfan Flowfields," AIAA Paper 90-3034, Aug. 1990.

[11]Boldman, D. R., Iek, C., Jeracki, R. J., Larkin, M., and Sorin, G., "Evaluation of Panel Code Predictions with Experimental Results of Inlet Performance for a 17-Inch Ducted Prop/Fan Simulator Operating at Mach 0.2," AIAA Paper 91-3354, June 1991.

[12]Larkin, M. J., and Schweiger, P. S., "Ultra High Bypass Nacelle Aerodynamics: Inlet Flow-Through High Angle of Attack Distortion Test," NASA CR-189149, July 1992.

[13]Cooper, G. K., and Sirbuagh, J. R., "The PARC Distinction: A Practical Flow Simulator," AIAA Paper 90-2002, July 1990.

[14]Steinbrenner, J. P., and Chawner, J. R., "Enhancements to the Gridgen System for Increased User Efficiency and Grid Quality," AIAA Paper 92-0662, Jan. 1992.

[15]Iek, C., Boldman, R. D., and Ibrahim, M., "Analysis of an Advanced Ducted Propeller Subsonic Inlet," AIAA Paper 92-0274, Jan. 1992.

[16]Horlock, J. H., "Actuator Disk Theory," McGraw-Hill, New York, 1978.

[17]Pinker, R. A., and Herbert, M. V., "Pressure Loss Associated with Compressible Flow Through Square-Mesh Wire Gauges," *Journal Mechanical Engineering Science*, Vol. 9, No. 1, 1967, pp. 11–23.